Experiments in Fluids 20 (1995) 42–55 © Springer-Verlag 1995

Turbulent expansion flow of low molecular weight shear-thinning solutions

O.S. Castro, F.T. Pinho

Abstract A Laser-Doppler anemometer and a pressure transducer were used to carry out detailed measurements of the mean and root mean square of the velocity and wall-pressure in an axisymmetric sudden expansion flow, with 0.4 and 0.5% by weight shear-thinning aqueous solutions of a low molecular weight polymer (6,000), after appropriate rheological characterisation. In spite of their very low molecular weight, these solutions still exhibited elongational elastic effects through drag reduction of up to 35% relative to Newtonian turbulent pipe flow, as shown by Pereira and Pinho (1994).

The results showed small variations of the recirculation bubble length with polymer concentration and Reynolds number and reductions of the normal Reynolds stresses of up to 30%, especially in the tangential and radial directions. The reduction in normal Reynolds stresses within the shear layer is an elongational elastic effect, but this elasticity needs to be considerably more intense, such as with high molecular weight polymers, in order to strongly affect the mean flow characteristics. The observed mean flow patterns with these low molecular weight polymer solutions were indeed similar to those exhibited by Newtonian and inelastic fluids.

Nomenclature

D	diameter of pipe downstream of sudden expansion
d	diameter of pipe upstream of sudden expansion
ER	expansion ratio
h	step height
K	consistency index in power law model
k	turbulent kinetic energy
L	recirculation bubble length
n	power law index in power law and Carreau viscosity models
R	radius of pipe downstream of sudden expansion
Re	Reynolds number
Re_a	Reynolds number based on wall viscosity in the upstream pipe
Re_{gen}	generalised Reynolds number (Eq. 4)
r	local radius
U	axial bulk velocity
U_{in}	axial bulk velocity at inlet
u	local axial mean velocity
u_0	axial centreline velocity
u'	local root mean square of axial velocity
v'	local root mean square of radial velocity
w'	local root mean square of tangential velocity
$\dot{\varepsilon}$	dissipation rate of turbulence
$\dot{\gamma}$	shear rate
λ	time constant of Carreau viscosity model
ρ	fluid density
μ	fluid viscosity
μ_a	viscosity at the wall in the upstream pipe
μ_0	zero shear-rate viscosity

Subscripts

ch	refers to a characteristic value
in	refers to characteristic values at the inlet pipe
max	refers to maximum values

Received: 14 December 1994/Accepted 11 July 1995

O. S. Castro,
Departamento de Engenharia Mecânica,
Instituto Superior de Engenharia do Porto,
Rua de S. Tomé, 4200 Porto, Portugal

F. T. Pinho
Departamento de Engenharia Mecânica e Gestão Industrial,
Faculdade de Engenharia da Universidade do Porto,
Rua dos Bragas, 4099 Porto Codex, Portugal

The authors acknowledge the support of the ex-Instituto Nacional de Investigação Científica – INIC, Instituto de Engenharia Mecânica e Gestão Industrial – INEGI and Laboratório de Hidráulica da Faculdade de Engenharia in helping to finance the rig, lending some equipment and for providing building space for the installation, respectively. We also would like to thank M. Paulo Coelho and Ms. Doris Dobbelman for their contribution to the measurements and Hoechst, Portugal for providing us with some of the polymer additives.

This paper is dedicated to the memory of late Professor A.O. Restivo

1 Introduction

The characteristics of non-Newtonian turbulent flows are still poorly understood, especially regarding wall-free behaviour. Early attempts at the investigation of wall-free non-Newtonian turbulent flows have mostly concentrated on the behaviour of very dilute polymer solutions of constant viscosity, which are known to exhibit drag reduction in turbulent wall flows. Berman and Tan (1985) and Koziol and Glowacki (1989) were among those few and they studied the flow of aqueous solutions of polyethylene oxide, showing the delay in jet spreading

together with a reduction in radial turbulence. However, the effects of many other rheological characteristics, such as variable viscosity and different types and magnitudes of elasticity continue to need proper investigation.

The wall-free shear layer resulting from the interaction of a jet and a recirculation bubble downstream of a sudden expansion flow makes this simple geometry suitable for investigation of wall-free turbulent flow characteristics. It also possesses important features that can be found in other more complex and more practical flows, so that it has become a much studied flow in Newtonian fluid mechanics, thus providing a wealth of data for comparative analysis and the validation of numerical codes.

Therefore, the sudden expansion is a suitable flow geometry for a thorough investigation of non-Newtonian wall-free turbulent flows. The requirements of a small rig and low quantities of fluid, which need frequent substitution due to fluid degradation, points out to its axisymmetric version as the simplest and most adequate for the investigation of non-Newtonian flows.

Newtonian sudden expansion flows have been thoroughly investigated in the past, in both the planar and axisymmetric geometries. The early measurements indicated that, at transitional Reynolds numbers much earlier than the appearance of turbulence, the flow became asymmetric, as demonstrated by Cherdron et al. (1978) and Iribarne et al. (1972), respectively. Then, according to the measurements of Abbott and Kline (1962) and Restivo and Whitelaw (1978) amongst others, it becomes symmetric again at higher Reynolds numbers, corresponding to turbulent flow.

Early experimental research on Newtonian axisymmetric sudden expansion flows in the laminar and transitional flow regimes were reported by Kalinske (1946), Macagno and Hung (1966), Iribarne et al. (1972) and Back and Roschke (1972), who relied on photographic and visualisation techniques. They showed the direct linear dependence of eddy size on Reynolds number and the effect of expansion ratio on the mean flow characteristics. It was also clear from these works that the inlet condition strongly influenced the flow downstream of the expansion, with fully developed inlet flows leading to longer recirculation bubbles than uniform and almost uniform velocity profiles.

Early attempts to measure turbulence fields with hot-wire by Freeman (1975) and Moon and Rudinger (1977) faced the enormous difficulties in using this technique within recirculating flows, which was surpassed by the use of new techniques, such as the pulsed-wire and the laser-Doppler anemometers.

The works of Khezzar et al. (1985), Durrett et al. (1988), Dimaczek et al. (1989) and Stieglmeier et al. (1989) were aimed at investigating Newtonian turbulent flow characteristics and reported recirculation bubble sizes, normalised by the step height, of up to 24 for inlet Reynolds numbers of 900, decreasing to values between 8 and 10 for Reynolds number above 2,000. These authors showed, for various conditions, maximum normal Reynolds stresses occurring downstream of the expansion within an annular region centred about the expansion radius. They also reported that the maximum values of the two transverse components of the normal Reynolds stresses occurred later than the maximum axial normal Reynolds stress. A second region of high turbulence was the end of the reattachment zone, because of the transport of turbulence by the mean flow and the production of turbulence by decelerating normal strain-normal stress interaction, as reported before by Cherry et al. (1984) for the planar geometry.

The literature on non-Newtonian expansion flows has been scarcer, especially regarding transitional and turbulent flow conditions. Halmos and Boger (1975) measured mean velocity and reattachment lengths in a 1:2 sudden expansion by means of a visualisation technique with an inelastic shear-thinning solution and for generalised Reynolds numbers below 150. Eddy size was shown to increase with Reynolds number, as happens with Newtonian fluids, and with shear-thinning intensity. These results, and their Newtonian counterpart, were also numerically predicted by Halmos et al. (1975) using a power law Ostwald-de Waele viscosity model. Perera and Walters (1977) were among the firsts to investigate the role of elasticity in their expansion/contraction/expansion laminar duct flow numerical simulations and predicted a reduction of the eddy size. This role of elasticity has been recently confirmed in the experiments and predictions of Townsend and Walters (1994) for two and three dimensional sudden expansions at low, laminar, Reynolds numbers. Given the fluids and the low Reynolds numbers flows that were investigated, such effect can be attributed to the shear elasticity of the fluids rather than to their elongational elasticity. These authors also reported a surprising lengthening of the recirculation bubble for fibre suspensions at similar flow conditions.

The recent experimental investigation of Newtonian, purely viscous and elastic shear-thinning sudden expansion flows of Pak et al. (1990), who also used a visualisation technique, confirmed that elasticity reduced the recirculation bubble size in laminar flow, but increased it in the turbulent regime. In the laminar regime the polymer concentration did not influence the eddy size of inelastic fluids, but for the viscoelastic case the bubble decreased with concentration, a clear sign of a stronger elastic effect. This work on elastic turbulent flows was further extended by Pak et al. (1991), who carried out measurements of axial pressure drop and mean velocity for two different expansion ratios and showed that elasticity reduced the pressure loss relative to an inelastic fluid. Unfortunately, these authors did not report, either rheological data on the type and intensity of elasticity of the fluids, or any Reynolds stresses, so that a complete picture of the flow field did not emerge from those two works.

In the confined baffle flow experiments of Pinho and Whitelaw (1991) with elongationally elastic shear-thinning fluids exhibiting drag reduction in turbulent pipe flow, a similar pattern of bubble size and pressure drop dependence on elasticity was observed and this was shown together with a damping of turbulence, especially in the radial and tangential components. Therefore, it is plausible that a similar behaviour occurred in the Pak et al. (1991) sudden expansion experiments.

It is clear from this review, that an extensive investigation of the turbulent and transitional sudden expansion flow characteristics with several non-Newtonian fluids of different rheology is required and this work is a contribution to such effort. Two different concentrations of an aqueous solution of a very low molecular weight polymer were selected and their mean and turbulent flow characteristics investigated in a sudden expansion flow.

Next, the fluid rheology, the flow configuration and instrumentation are described, and are followed by the presentation of the results and their discussion. This work ends with a summary of the main conclusions.

2 Fluid characteristics

The flow measurements were preceded by the selection of an appropriate shear-thinning fluid of low molecular weight from a set of candidate fluids, as described in Pereira and Pinho (1994). The fluids selected were aqueous solutions of the low molecular weight (6,000 kg/kmole) methyl hydroxyl cellulose, Tylose MH 10000K from Hoechst, at concentrations of 0.4 and 0.5% by weight. The polymer was dissolved in Porto tap water and the rheological characterisation was carried out with the Physica double gap concentric cylinder rheometer, model MC100. The viscosity of the solutions at 25 °C and its variation with the shear rate is plotted in Fig. 1 together with the simplified Carreau model (Eq. (1)) resulting from a curve fitting to the experimental data, whose parameters are listed in Table 1. The solutions were rheologically considered as inelastic as far as shear flows are concerned. Measurements of the shear elasticity material functions were difficult because the solutions were too dilute for the accuracy of the rheometer. However, creep and oscillatory tests were carried out with a more concentrated 0.6% by weight Tylose solution, and the results are presented in Figs. 2 and 3, respectively.

The ratio of the elastic reversible stored shear deformation to the viscous absorbed shear deformation in the creep test, shown in Fig. 2, was very small, i.e., below 0.3% for the applied shear stresses of 0.6 and 1.5 Pa. In the oscillatory shear tests it was not possible to get reliable data for amplitudes of deformation under 0.2, for which Fig. 3 shows the effect of the frequency of oscillation on the storage and loss moduli, G' and G'', respectively. The storage moduli is less than 10% of the loss modulus, this ratio dropping further for higher frequencies.

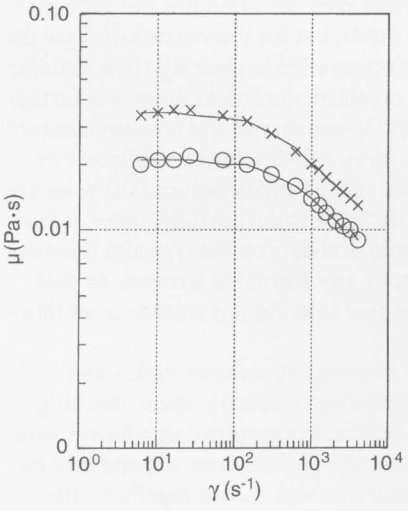

Fig. 1. Viscosity of the 0.4% (○) and 0.5% (×) Tylose solutions and Carreau model fitting at 25 °C [from Pereira and Pinho (1994)]

Table 1. Parameters of the Carreau model for the aqueous solutions of Tylose MH 10000 K at 25 °C

Solution	μ_0 [Pa.s]	λ [s]	n	$\dot{\gamma}$[s^{-1}]
0.4% Tylose	0.0208	0.0047	0.725	6.1 to 4031
0.5% Tylose	0.0344	0.005	0.660	6.1 to 4031

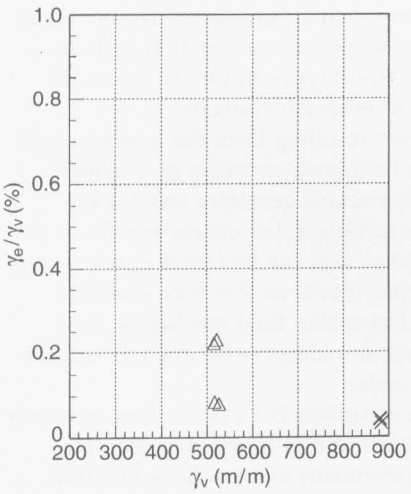

Fig. 2. Ratio of elastic to viscous deformation in the creep test of the 0.6% Tylose solution at 25 °C. Applied shear stresses: △ −0.6 Pa; × −1.5 Pa

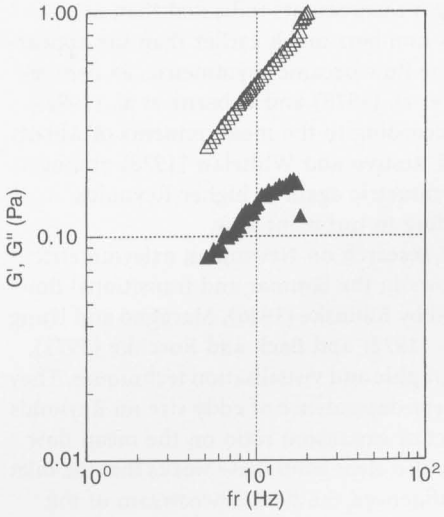

Fig. 3. Storage (▲) and loss (△) moduli (G', G'') of the 0.6% Tylose solution at 25 °C for an amplitude of deformation of 0.2

No elongational rheological tests were performed with these fluids, but the Tylose solutions were seen to be elongationally elastic, because they exhibited drag reduction in the turbulent pipe flow experiments described by Pereira and Pinho (1994), in spite of their shear rheology and of their low molecular weight. These pipe flow measurements in a 26 mm diameter pipe showed drag reductions of up to 35% relative to water flows at the same Reynolds numbers based on wall viscosity. The measured drag reduction was about half the maximum

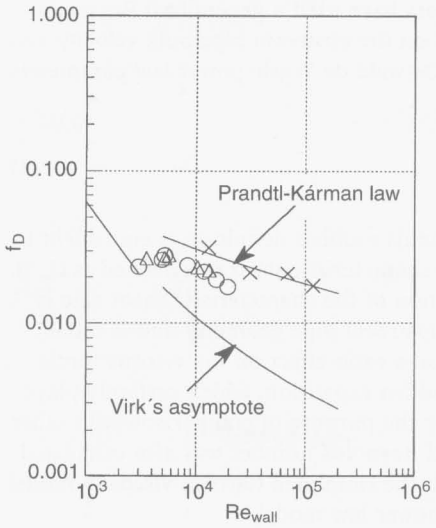

Fig. 4. Darcy friction factor versus wall Reynolds number [from Pereira and Pinho (1994)]. (×) water; (○) 0.4% Tylose; (△) 0.5% Tylose

drag reduction predicted by Virk's asymptote, Virk (1975), as can be confirmed in Fig. 4.

$$\mu = \mu_0 [1 + (\lambda \dot{\gamma})^2]^{(n-1)/2} \tag{1}$$

3
Flow configuration and instrumentation

The flow configuration, fully described in Castro (1994), is similar to that used in the pipe flow experiments of Pereira and Pinho (1994), except for the test section and the ensuing duct leading to the tank. The installation consisted of a vertical closed loop with a 100 l tank and a centrifugal pump located at the bottom of the rig. The descending 2.4 m long pipe had an internal diameter of 26 mm and ended at an abrupt sudden expansion to a 40 mm diameter pipe, thus defining a test section with an expansion ratio of 1.538. After this test section of 430 mm of length a further 700 mm long pipe of 40 mm diameter carried the fluid back to the tank. The test section, represented schematically in Fig. 5 with the coordinate system used throughout this test, had a square outer cross section to reduce diffraction of light beams. A honeycomb was placed at the inlet of the descending 26 mm pipe, i.e. ninety diameters upstream of the sudden expansion, to help ensure a fully developed turbulent pipe flow at the inlet of the test section, as confirmed by the measurements of Pereira and Pinho (1994).

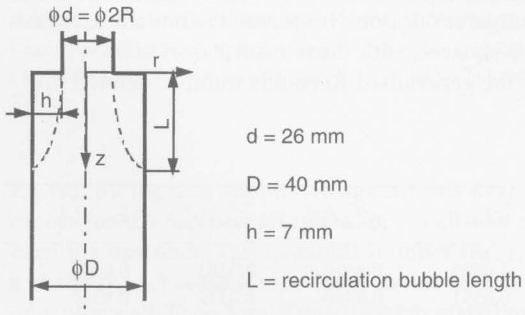

Fig. 5. Schematic representation of the test section, its dimensions and the coordinate system

Table 2. Laser-Doppler characteristics

Laser wavelength	827 nm
Laser power	100 mW
Measured half angle of beams in air	3.68
Measuring volume size in water (e^{-2} intensity)	
minor axis	37 mm
major axis	550 mm
Fringe spacing	6.44 mm
Frequency shift	2.5 MHz

Eleven pressure taps were drilled on the sudden expansion test section, but were not close enough to each other to provide detailed longitudinal pressure profiles, a task which will be reported in the near future. The flow rate was controlled by operating two valves and was monitored by the pressure variation between the two pressure taps, located before and after the sudden expansion, which showed the largest pressure difference as well as by the velocity measurements. The flow rate was calculated from the integrated velocity profiles at all measuring stations.

The above pressure drop was measured with a P305D Valydine differential pressure transducer, diaphragm number 30, which was interfaced with a 386 PC by a data acquisition Metrabyte DAS-8 board. The statistical quantities were calculated by purpose-built software and the overall uncertainty of the pressure measurements were better than 1.2 Pa, which is less than 2% for the flow rate range reported here.

A miniaturised fibre optics laser-Doppler velocimeter from INVENT, model DFLDA, was used for the velocity measurements with a 100 mm focusing lens mounted on the S-30 optical probe. Scattered light was collected in the forward direction by an avalanche photodiode and sent to a TSI 1990C counter for processing. The anemometer is fully described in Stieglmeier and Tropea (1992) and its main characteristics, of relevance to this work, are listed in Table 2. The output of the counter was sent, via a DOSTEK 1400A interface card, to a computer which provided the statistical quantities. The velocimeter was mounted on a milling table with movement in the three coordinates and the maximum velocity and positional uncertainties at a 95% confidence level are as follows: 2% and 3.1% on axis to 2.8% and 7.1% in the high turbulence region downstream of the sudden expansion for the axial mean and rms velocities, respectively; 4.1% and 9.4% on axis and in the high turbulence region for both the radial and azimuthal rms velocity components; 200 μm for the x and y horizontal positioning of the control volume and 140 μm in the longitudinal (vertical) positioning of the control volume. The effect of refraction of the laser beams at the curved optical boundaries was taken into account in the calculations of the measuring volume location and conversion factors, according to Durst et al. (1981).

4
Results and discussion

4.1
Definition of viscosity

In non-Newtonian fluid mechanics the definition of a Reynolds number is not as straightforward as in classical fluid

mechanics, because of the variation of viscosity with shear rate. For internal laminar flows in ducts of constant cross section area, there is now enough information indicating the advantages of a universal usage of the Kozicki Reynolds number defined by Kozicki et al. (1968), as shown by Kostic (1994b). However, for turbulent and more complex flows there is still no agreement on the best definition of Reynolds number.

In the particular case of the sudden expansion flow with fluids of constant viscosity, both the upstream diameter and step height have been used as characteristic lengths, with improved collapse of data when the former is used in the Reynolds number definition and the latter is used to normalise the eddy length. For variable viscosity fluids it is also necessary to define an apparent viscosity, which should represent as faithfully as possible an average value that is characteristic of the viscous processes taking place within the flow. So, it seems that the appropriate definition of a Reynolds number for this flow is of the type

$$Re = \frac{\rho U_{in} d}{\bar{\mu}(\dot{\gamma}_{ch})} \tag{2}$$

Viscosity plays a role in the dissipation of turbulent kinetic energy in turbulent flows and the following definition of viscosity was derived for power law fluids by Politis (1989), who considered the effect of the fluctuating velocities upon the average shear rate used to calculate the average viscosity.

$$\bar{\mu} = \rho^m K^{1-m} \dot{\varepsilon}^m \exp\left[m(m-1)\sigma^2/2\right] \tag{3}$$

K and n are the power law parameters, $\dot{\varepsilon}$ is the turbulent dissipation rate, $m = (n-1)/(n+1)$, $\sigma^2 = 0.45 \ln(L/\eta)$ where L and η represent the macro and micro scales of turbulence, respectively.

In spite of its sound physical basis, this expression is rather complex, requires an *a priori* detailed knowledge of the mean and turbulent flow fields and consequently makes it difficult to compare different experiments; therefore, a different approach will be used here.

Removing the effect of the fluctuating velocity field, the characteristic shear rate in the mixing layer ($\dot{\gamma}_{ch}$) downstream of the sudden expansion is, on average, proportional to the ratio of the upstream mean velocity (U_{in}) to the step height (h):

$$\dot{\gamma}_{ch} = \frac{U_{in}}{h} = \frac{2U_{in}}{d(ER-1)} \tag{4}$$

Equation (4), together with the simplified Carreau model for the viscosity (Eq. (1)), defines the average viscosity $\bar{\mu}$ used in the Reynolds number (Re), throughout this paper. The characteristic length will be again the upstream diameter d, as in Newtonian fluid mechanics.

Previous investigators have used a generalised Reynolds number (Re_{gen}) based on the upstream pipe bulk velocity and diameter and on the Ostwald de Waele power law parameters K and n.

$$Re_{gen} = \frac{\rho d^n U_{in}^{2-n}}{K} \tag{5}$$

This generalised Reynolds number definition is equivalent to using Eq. (2), with the characteristic shear rate defined as U_{in}/d. Obviously, this definition of the characteristic shear rate is purely based on the upstream pipe geometry and is independent of the expansion ratio effect on the viscous forces downstream of the sudden expansion, which certainly plays a specific role. Just for the purpose of comparison with other works this generalised Reynolds number was also calculated here, but coupled with the simplified Carreau viscosity model rather than with the power law model.

4.2 Mean flow

Three flow conditions, corresponding to the maximum flow rates for water, 0.4 and 0.5% by weight Tylose solutions, were thoroughly measured and compared. In order to investigate the Reynolds number effect, the 0.4% solution was also measured at a lower flow rate corresponding to a similar Reynolds number as the 0.5% Tylose solution at the maximum flow rate. The main characteristics of these four tests are summarised in Table 3, which lists the upstream bulk velocity, the two flow Reynolds numbers, the normalised recirculation length, the normalised maximum normal Reynolds stresses and the normalised maximum turbulent kinetic energy. The turbulence data of Table 3 are maximum turbulence values and do not necessarily occur at the same location within the flow.

To measure the recirculation bubble length the axial velocity was measured twice in a fine grid around the estimated location of the flow reattachment and the data interpolated. The nodes of this grid were spaced axially and radially by 3 and 0.2 mm, respectively and the overall uncertainty of the eddy size measurement, due to the measuring volume positioning and the mean velocity measurement accuracies, was better than 5%.

Figure 6 compares well our normalised recirculation length for Newtonian fluid flows with that of other researchers for different expansion ratios. It is clear that the variation of bubble length for Reynolds numbers above 5,000 is minimum. There is a small expansion ratio effect in the slightly lower normalised eddy sizes for the lower expansion ratios.

Figure 7 compares our non-Newtonian recirculation lengths, represented as squares, with those from Pak et al. (1990) as a function of the generalised Reynolds number defined in

Table 3. Main flow characteristics of water and Tylose flows

Fluid	U_{in} [m/s]	Re	Re_{gen}	L/h	$\overline{u'^2_{max}}/U_{in}^2$	$\overline{w'^2_{max}}/U_{in}^2$	$\overline{v'^2_{max}}/U_{in}^2$	k_{max}/U_{in}^2
Water	6.09	178,000	178,000	8.67	0.0506	0.0326	0.0281	0.0542
0.4% Tyl	4.60	7,950	6,180	8.44	0.0551	0.0350	0.0252	0.0567
0.4% Tyl	6.45	12,150	9.070	8.00	0.0471	0.0280	0.0199	0.0476
0.5% Tyl	6.06	7,600	5,300	8.65	0.0534	0.0295	0.0206	0.0487

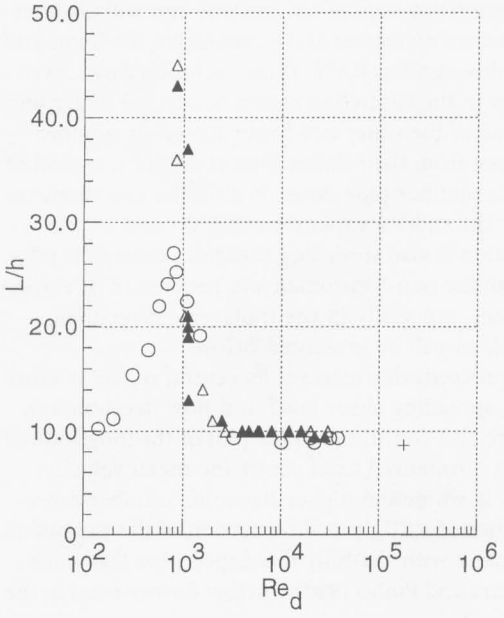

Fig. 6. Normalised recirculation bubble length for Newtonian fluids. (○) $D/d = 1.749$, Khezzar (1985); (△) $D/d = 2.0$, Pak et al. (1990); (▲) $D/d = 2.667$, Pak et al. (1990); (+) $D/d = 1.538$ present work

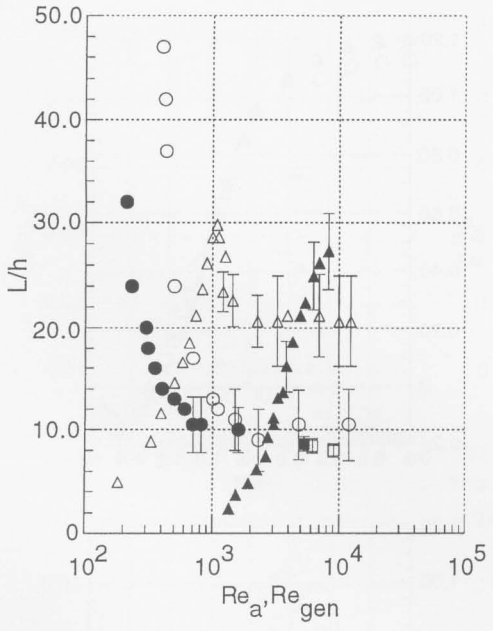

Fig. 7. Normalised recirculation bubble length for non-Newtonian fluids (comparison with Pak et al. (1990)). $D/d = 2.667$: (○) 5000 ppm Carbopol; (●) 15,000 ppm Carbopol. $D/d = 2.0$: (△) 200 ppm Separan; (▲) 1000 ppm Separan. $D/d = 1.538$: (□) 0.4% Tylose; (■) 0.5% Tylose

Eq. (4). All the data are plotted against this Reynolds number, except for the Separan solutions for which Pak et al. (1990) used the upstream wall Reynolds number (Re_a), based on a viscosity (μ_a) calculated at the upstream wall shear rate at the inlet pipe wall. Therefore, if one wants to make comparisons on the basis of Re_{gen} the two curves pertaining to Separan in Fig. 7 must be shifted to the left, i.e., the upstream wall Reynolds number values are higher than the corresponding generalised Reynolds number values.

The Newtonian flow results of Fig. 6 show no major difference between ours and the measurements of Pak et al. (1990), whereas in the shear-thinning plots of Fig. 7 the Tylose solutions exhibit slightly shorter eddy sizes than those of Pak et al.'s Carbopol solutions, and much smaller than their results for the strongly viscoelastic polyacrylamide solutions. Pak et al. (1990) considered their Carbopol solutions as purely viscous based only on standard rheometrical data. They report neither the friction factor data in turbulent pipe flow with their Carbopol solutions, not any normal Reynolds stress measurements in the sudden expansion flow, which would give more insight into this flow and fluid. Similar Carbopol solutions have been previously reported as elastic fluids under shear, but also known to exhibit no drag reduction in turbulent pipe flows (Kostic 1994a). However, as this work attempts to show, the elongational elasticity that affects both the mean and the turbulent flow of the polyacrylamide solutions of Pak et al. (1990) can also be responsible for an effect on turbulent flow characteristics only, without a detectable effect upon the mean flow, as happens with the Tylose solutions here.

For the Tylose solutions, on the contrary, despite its low molecular weight and the fact that the rheological measurements were unable to detect a sizeable elasticity in shear flows, the turbulent pipe flow measurements of Pereira and Pinho (1994) showed drag reduction, an indication of a strong elongational elasticity effect. These results, together with the above mentioned behaviour of Carbopol (Kostic 1994a), are clear evidences that standard rheometrical measurements are not enough to characterise the elastic behaviour of non-Newtonian solutions under turbulent flow conditions, such as drag reduction in pipe flow. The drag reduction phenomena is a consequence of the increased elongational viscosity brought about by molecular stretching (Hinch 1977; Kostic 1994a), whereas standard rheological measurements of elasticity are aimed at the behaviour of the solutions under shear, where the molecules are at conditions close to equilibrium. The inexistence of commercially available elongational rheometers for dilute solutions led us to quantify elongational elasticity effects indirectly, as pressure drop versus Reynolds number correlations in turbulent flow pipe (Pereira and Pinho 1994).

Table 3 shows a slight reduction of eddy size with the addition of 0.4% Tylose to water at the maximum flow rate, accompanied by an increase in viscosity and a lower Reynolds number. As clearly depicted in Fig. 6 with Newtonian fluids, for Reynolds numbers below 4,000 a decrease in Reynolds number is accompanied by the lengthening of the recirculation bubble as one moves into the transitional regime, a behaviour also exhibited by the 0.4% Tylose solutions, although at higher Reynolds numbers. This is not an unusual behaviour with non-Newtonian fluids; delays in transition due to non-Newtonian fluid behaviour have been reported in the past by Hoyt (1972) and Pinho and Whitelaw (1991) amongst others. However, since the Reynolds number of the maximum bulk velocity 0.4% Tylose flow is much higher than the 4,000 limit, any variation in eddy size between the water and the Tylose flow must be attributed to a different cause, namely a change in fluid rheology. Then, adding more polymer to the 0.4% Tylose flow, up to 0.5%, at maximum flow rate increases the bubble

length and this variation results from two different effects acting in the same direction: a higher polymer concentration increases the elasticity of the fluid, which lengthens the bubble, and increases its viscosity thus lowering the Reynolds number in a range where transitional effects may start to be taking place, especially because non-Newtonian elastic fluids are known to widen the transitional flow regime range. At first sight these variations could be considered meaningless due to their small magnitude and in comparison to the measuring uncertainties, but Pinho and Whitelaw (1991) have also observed similar variations of the recirculation bubble length in their baffled flow experiments with the more elastic CMC solutions. They reported a reduction in eddy length by adding 0.1% CMC to water at Reynolds numbers above 20,000, followed by a recirculation bubble increase with further addition of polymer at Reynolds numbers well above those used here. So, in both instances the addition of polymer to water reduced the bubble length; this took place at high Reynolds numbers and the evidence indicates that it is a rheological effect but the authors can not yet explain it.

The radial profiles of the normalised axial mean velocity at several downstream stations of Fig. 8a–f include Reynolds number and polymer concentration effects. The profiles are not very different from each other, but one can still see that within two upstream diameters of the expansion, the water and the high Reynolds number 0.4% Tylose solution flows have velocity profiles in the centreline region which are flatter and wider than those of the other two lower Reynolds number flows, as expected from their flatter inlet conditions, typical of higher Reynolds number pipe flows. Within the first diameter downstream of the sudden expansion (Fig. 8b and c), the turbulent diffusion is also spreading the water centreline jet at a faster rate than the non-Newtonian jets, because of its earlier higher turbulence, especially in the transverse directions (Fig. 11 and 12), as will be presented below.

As the flow proceeds downstream its central region is more affected by the spreading shear layer and flow deceleration. These effects are also confirmed in the plot of the longitudinal variation of the normalised axial centreline mean velocity (u_0/U_{in}) in Fig. 9, where the higher Reynolds number flows show lower values of u_0/U_{in} just downstream of the expansion again in agreement with the fully developed pipe flow inlet condition (Pereira and Pinho 1994). Further downstream in the recovery region, the normalised centreline velocity for the water and the high Reynolds number 0.4% Tylose flows again tend to lower asymptotic values than the other two flows, as

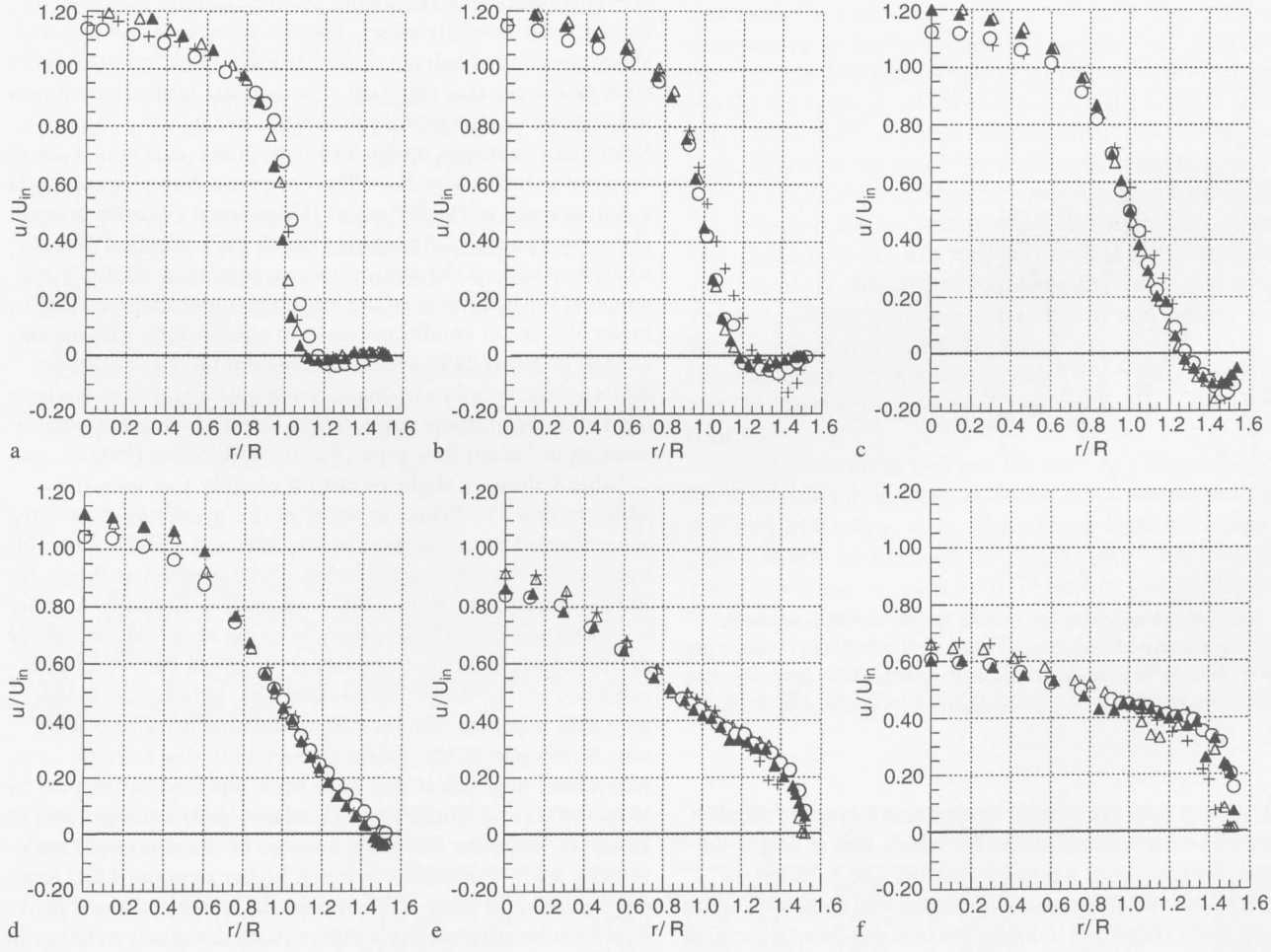

Fig. 8a–f. Radial profiles of normalised axial velocity for (+) water $Re = 178{,}000$; (△) 0.4% Tylose $Re = 7{,}950$; (○) 0.4% Tylose $Re = 12{,}150$; (▲) 0.5% Tylose $Re = 7{,}600$, at **a** $0.25D$, **b** $0.5D$, **c** $1.0D$, **d** $2.0D$, **e** $4.0D$ and **f** $6.0D$.

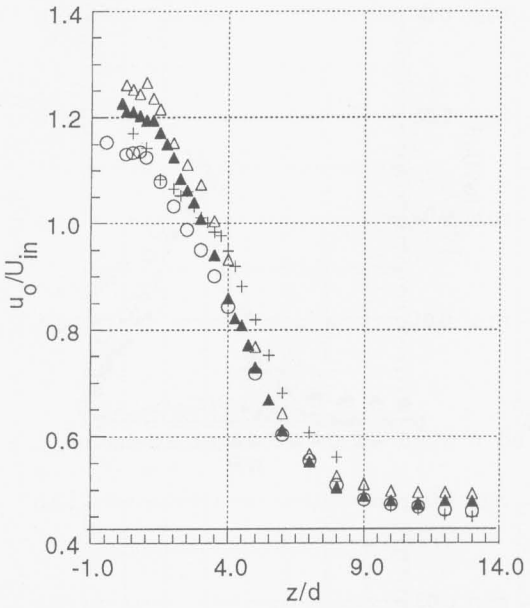

Fig. 9. Longitudinal variation of axial velocity. (+) water $Re = 178{,}000$; (△) 0.4% Tylose $Re = 7{,}950$; (○) 0.4% Tylose $Re = 12{,}150$; (▲) 0.5% Tylose $Re = 7{,}600$

expected and observed in the inlet pipe. The full line in Fig. 9 represents the ratio of the downstream to the upstream bulk velocities.

4.3 Turbulent flow

The maximum normal Reynolds stresses and turbulent kinetic energy for each flow condition are also listed in Table 3, again showing polymer concentration and Reynolds number effects.

Figures 10 to 12 show radial profiles of the normalised axial, tangential and radial normal Reynolds stresses at some selected locations, whereas Fig. 13 shows the complete mapping of these quantities via contour plots which include data from other measuring stations. Just after the sudden expansion (Figs. 10, 11, 12a and b) the turbulence levels of the low Reynolds number flows are higher than those of the water and high Reynolds number 0.4% Tylose flow. This agrees with the higher inlet turbulence (Fig. 10a) typical of low Reynolds number fully developed pipe flow (Pereira and Pinho 1994) especially close to the wall and, for these flows, it also includes the effect of some shear-layer flapping. For instance, at $0.25D$ the probability distribution function of u' for the 0.5% Tylose flow at the shear layer (around $r/R = 1.0$) showed a bimodal

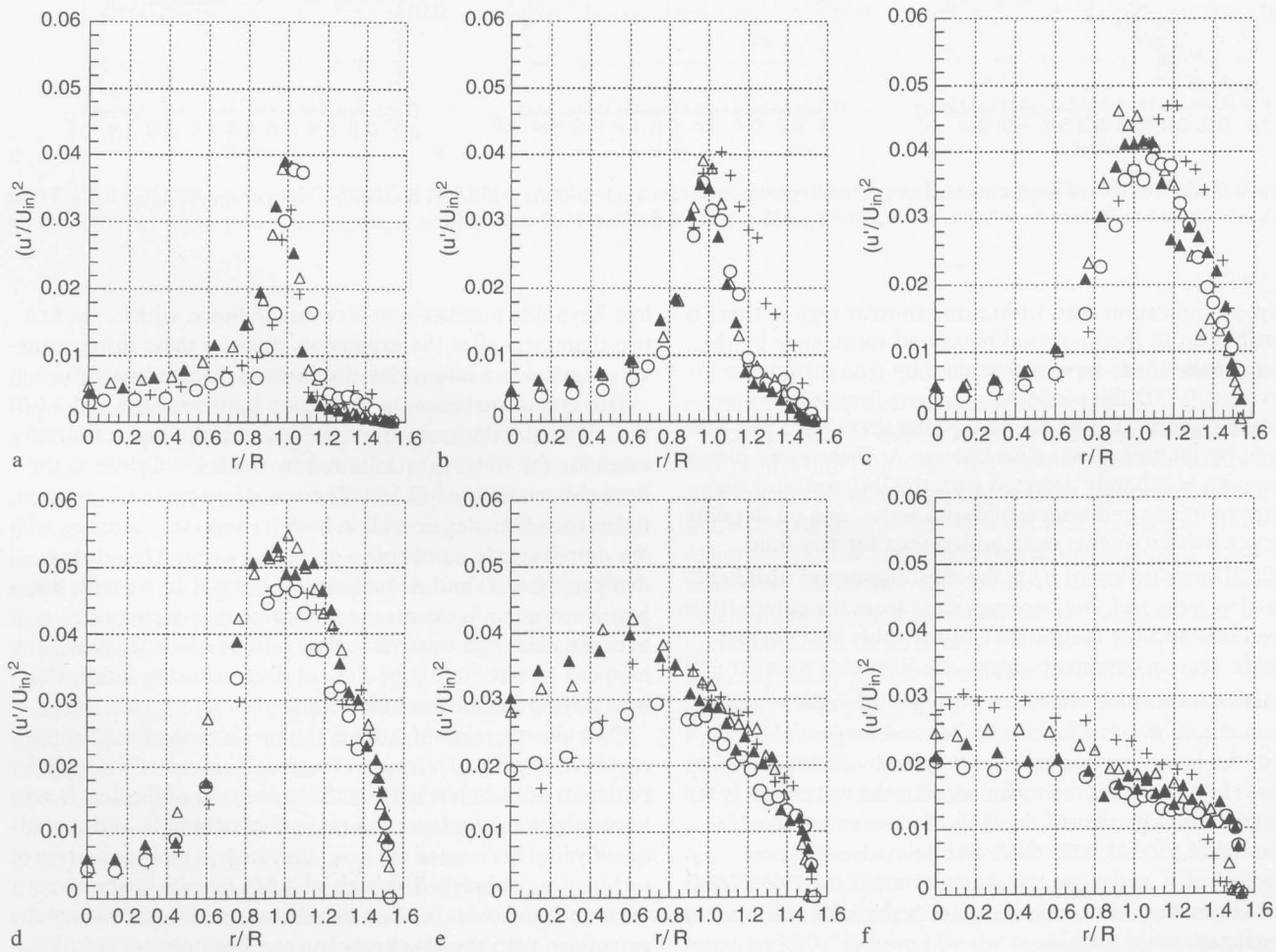

Fig. 10a–f. Radial profiles of the normalised axial Reynolds stress for (+) water $Re = 178{,}000$; (△) 0.4% Tylose $Re = 7{,}950$; (○) 0.4% Tylose $Re = 12{,}150$; (▲) 0.5% Tylose $Re = 7{,}600$, at **a** $0.25D$, **b** $0.5D$, **c** $1.0D$, **d** $2.0D$, **e** $4.0D$ and **f** $6.0D$

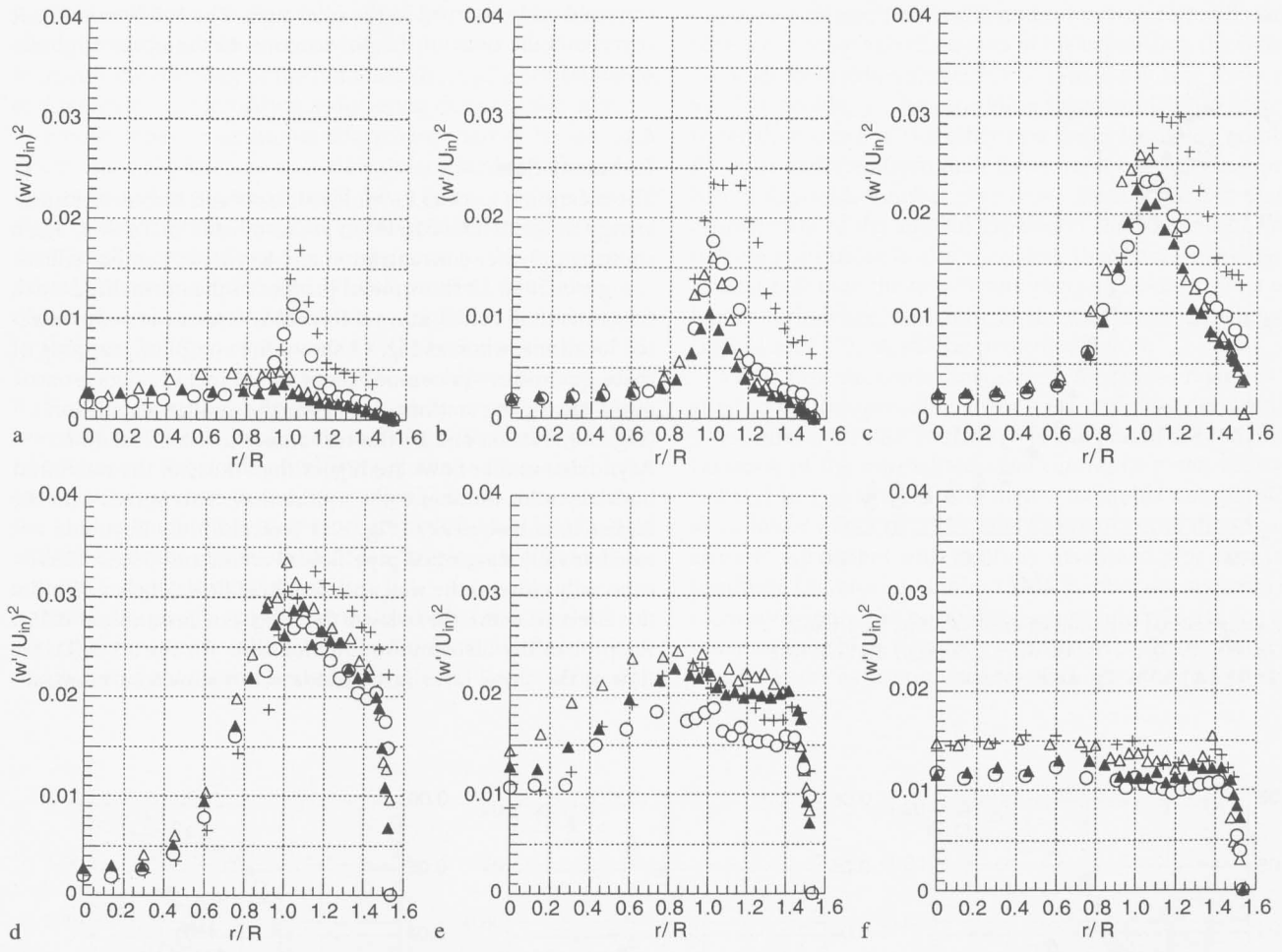

Fig. 11a–f. Radial profiles of the normalised tangential Reynolds stress for (+) water $Re = 178{,}000$; (△) 0.4% Tylose $Re = 7{,}950$; (○) 0.4% Tylose $Re = 12{,}150$; (▲) 0.5% Tylose $Re = 7{,}600$, at **a** $0.25D$, **b** $0.5D$, **c** $1.0D$, **d** $2.0D$, **e** $4.0D$ and **f** $6.0D$

pattern, an indication that, within this annular region, there is a contribution to the increased measured turbulence by the flapping of the shear-layer rather than by true turbulence. However, at $0.75D$ the probability density function was not bimodal anymore, i.e., the flapping of the shear layer was now smeared by the turbulence fluctuations. At these same places the flapping was barely detected with the less concentrated polymer solutions and undetected with water, and no flapping frequency measurements were undertaken for any fluid.

At $0.25D$ production of $\overline{u'^2}$ is the most important turbulence production term and this becomes clear from the comparison between this and the magnitudes of the other two normal Reynolds stress components. Here, the Reynolds number and polymer concentration effects are stronger upon the $\overline{v'^2}$ and $\overline{w'^2}$ components (Figs. 11, 12a); the radial and tangential turbulence of the low Reynolds number flows are still unaffected by the shear layer whereas the turbulence for the water flow is the highest followed by that of the 0.4% Tylose at a Reynolds number of 12,150. At $0.5D$ there has been already some production of v' and w' at the shear layer for the 7,600/7,950 Reynolds number flows, but the water turbulence still reaches values almost twice as large.

The spreading of turbulence and of the shear layer into the recirculation zone is faster with the water flow than with the low Reynolds number non-Newtonian flows, within the first two diameters after the expansion, because these lower transverse turbulence intensities also mean less turbulent diffusion.

Further downstream, in the region between $2.0D$ and $3.0D$, turbulence reaches maximum values with the highest intensities for the water flow followed by the 0.4% Tylose at the Reynolds number of 12,150. The non-Newtonian effect upon turbulence shows again well in both transverse quantities, with the more intense dampening occurring on v'. This strong dampening in v' and w' turbulence, but not in u', with the non-Newtonian fluids means that there is a decoupling between axial and transverse fluctuations of velocity, as happens in turbulent pipe flow of drag reducing fluids, thus intensifying turbulence anisotropy.

Only downstream of $2.0D$ is the turbulence in the central region of the flow starting to increase because of the radial transport of turbulence. Now, the turbulence of the flow is very intense in the shear layer and recirculation bubble, and spreads quickly into the core of the flow. Curiously, a strange pattern of turbulence is observed at around $4.0D$; despite lower transverse turbulence in the first two diameters downstream of the expansion with the low Reynolds number polymer solution flows, the turbulence in the centreline region at $4.0D$ becomes higher with these flows than with the higher Reynolds number

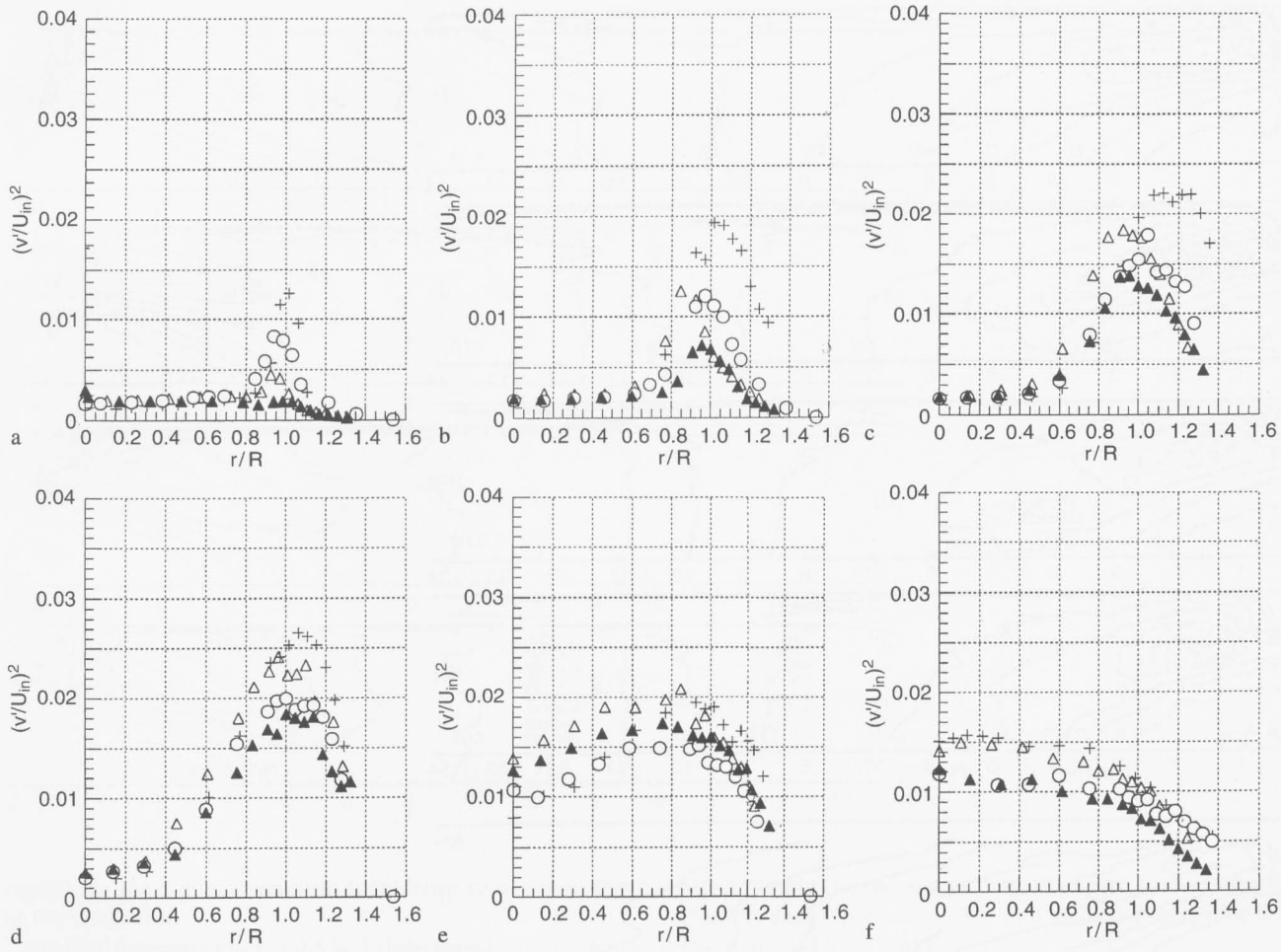

Fig. 12a–f. Radial profiles of the normalised radial Reynolds stress for (+) water $Re = 178{,}000$; (△) 0.4% Tylose $Re = 7{,}950$; (○) 0.4% Tylose $Re = 12{,}150$; (▲) 0.5% Tylose $Re = 7{,}600$, at **a** $0.25D$, **b** $0.5D$, **c** $1.0D$, **d** $2.0D$, **e** $4.0D$ and **f** $6.0D$

flows. This is well shown in the contour plots of normal Reynolds stresses of Fig. 13, which were included to provide a better of overall picture of the turbulence flow field.

Figure 13 shows that in the shear layer region the contours are more elongated longitudinally for the high Reynolds number flows, whereas at low Reynolds numbers they are bent towards the centreline region. The figure also shows that this is mainly due to the highest turbulence levels of these latter flows in the central part of the inlet duct, which is being convected downstream. However, the authors do not believe this to be the only reason.

At lower Reynolds numbers the authors observed some flow unsteadiness, especially at the stations downstream of $2.0D$, which showed up through flow asymmetry and higher velocity fluctuations. This is a characteristic behaviour of low Reynolds number flows within the transitional regime and it has been observed previously by Pinho and Whitelaw (1991) in their CMC baffle flow. It is possible that this unsteadiness still persists at Reynolds numbers around 8,000 although very much smeared by the high turbulence. Due to difficulties in controlling the flow rate in the rig between different days, because of the lack of a by-pass and a flow meter, this effect was not further investigated, but remains as one of our future research aims in sudden expansion flows.

Downstream of $4.0D$ the mean velocity gradients are small and production of turbulence becomes less relevant, with dissipation of turbulence playing a more important role. The more intense dissipation with the non-Newtonian fluids, together with the above mentioned decoupling of axial and transverse turbulence and the consequent increase in turbulence anisotropy means that the turbulence levels in these non-Newtonian flows decays faster than those of the water flow, especially for the transverse components.

The contour plots of Fig. 13 confirm the previous described Reynolds number and polymer concentration effects and quickly illustrate the main turbulence tendencies: addition of 0.4% Tylose to water, for the maximum flow rate, reduces both the maximum values of the Reynolds stresses and the turbulence everywhere in the flow field, especially in the two transverse directions. The radial component of turbulence is the most affected, with a decrease of the maximum value of up to 30%, followed by the tangential and axial components with reductions of up to 14 and 7%, respectively. The turbulence is again raised with both a further addition of

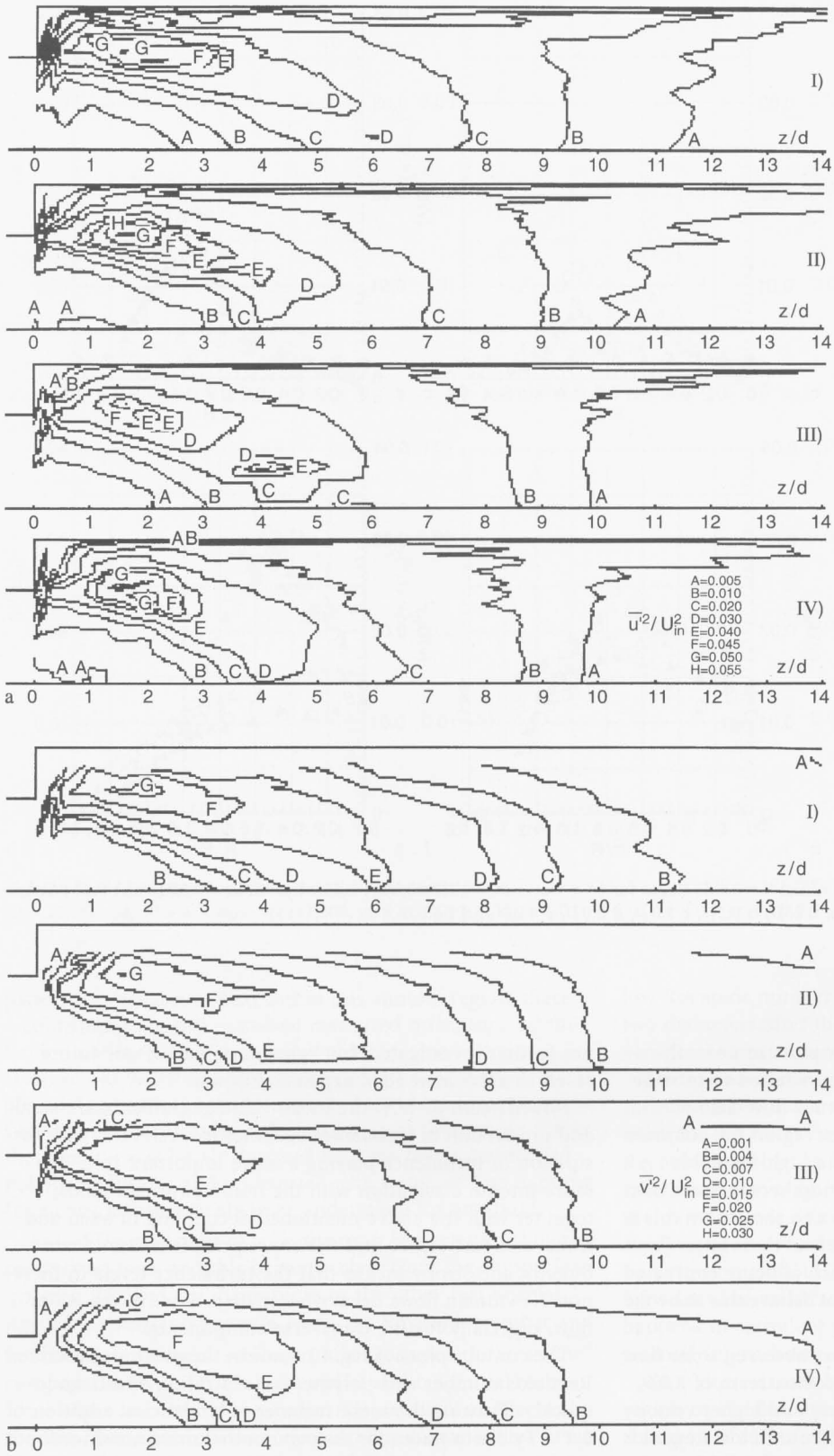

Fig. 13. **a** Contours of the normalised axial normal Reynolds stress. (I) Water $Re = 178{,}000$ (II) 0.4% Tylose $Re = 7{,}950$ (III) 0.4% Tylose $Re = 12{,}150$ (IV) 0.5% Tylose $Re = 7{,}600$; **b** contours of the normalised normal radial Reynolds stress. (I) Water $Re = 178{,}000$, (II) 0.4% Tylose $Re = 7{,}950$, (III) 0.4% Tylose $Re = 12{,}150$, and (IV) 0.5% Tylose $Re = 7{,}600$; **c** contours of the normal tangential Reynolds stress. (I) Water $Re = 178{,}000$, (II) 0.4% Tylose $Re = 7{,}950$, (III) 0.4% Tylose $Re = 12{,}150$, (IV) 0.5% Tylose $Re = 7{,}600$

polymer concentration to 0.5% and a flow rate reduction with the 0.4% solution, because the Reynolds number decreases and the flow enters the transitional regime. In the shear layer that forms between the recirculation bubble and the jet coming from the upstream pipe, within the neighbourhood of the sudden expansion, the turbulence for the low Reynolds number flows is raised by shear layer flapping, as shown by the bimodal probability distribution functions of the velocity, thus

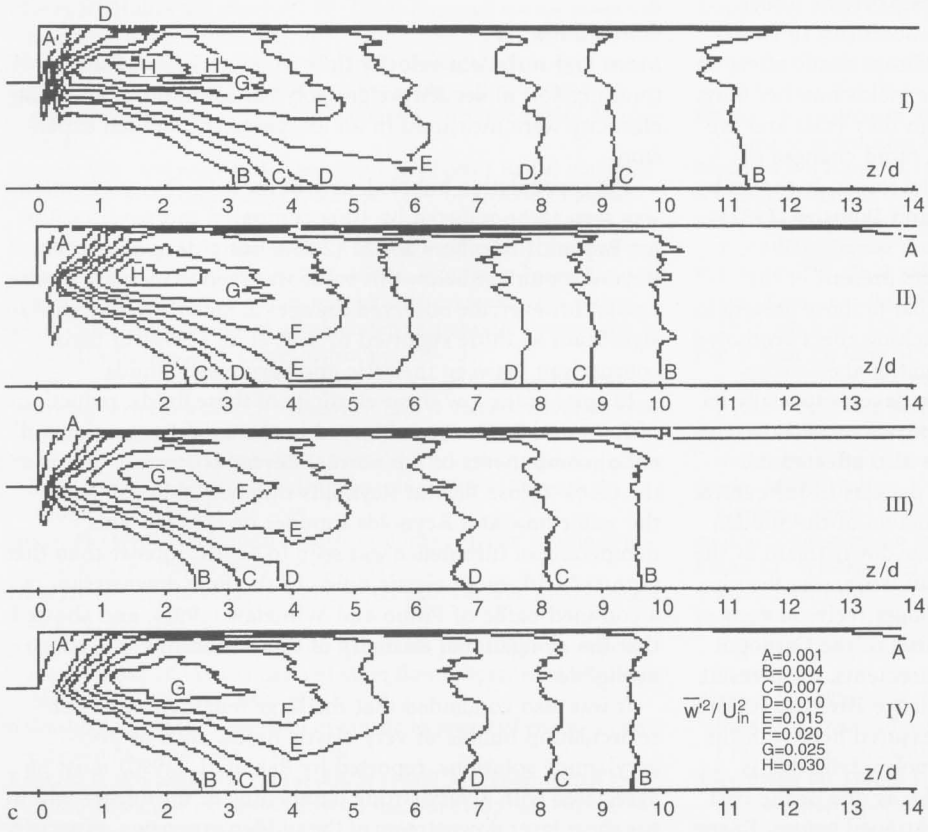

Fig. 13 (Continued)

explaining the higher maximum turbulence values than those of the water flow.

Further downstream, the 0.5% Tylose flow has turbulence levels already similar to those of the 0.4% Tylose at a Reynolds number of 12,250, in spite of the earlier higher turbulence. The dissipation of axial turbulence is faster with both shear-thinning fluids than with the water, so that the non-Newtonian flows already show less axial turbulence downstream of $z/d = 5$. In all the other comparisons between the different flow conditions, the variations of the maximum values of turbulence listed in Table 3 are similar to the variations in the overall turbulent flow field, i.e., lower maximum values of turbulence are accompanied by lower turbulence at other equivalent locations. A reduction of Reynolds number at a constant Tylose concentration of 0.4% leads to higher turbulence and the increase in polymer concentration from 0.4 to 0.5% at a constant Reynolds number of 7,800 reduces turbulence. It is also important to remark that these variations of turbulence with Reynolds number and polymer concentration are consistent with the eddy size changes, even though these are small.

The dampening of turbulence with the low elasticity Tylose solutions investigated here is less intense than that reported to occur with the more elastic CMC flows downstream of a confined baffle, especially in the axial and tangential directions, where maximum turbulence reductions of 20 and 40% were measured by Pinho and Whitelaw (1991) between Newtonian and the 0.2% CMC flows at a constant Reynolds number of 8,000, and of 13% and 21% between the 0.2% and 0.4% CMC solutions, respectively.

The strong dampening of transverse turbulence shown here is another sign of elongational elasticity, which is known to affect mainly the radial and tangential directions, in both wall (Luchik and Tiederman 1988) and wall-free turbulent flows (Berman and Tan 1985).

The differences between the mean flow data of the Tylose solutions and the measurements of Pak et al. (1990) with Carbopol are small and have no meaning at first sight, because of the uncertainties of the measurements of bubble length in both works and of the different inlet conditions; whereas they had a settling chamber followed by a contraction just upstream of the sudden expansion, in the present work there is a 90 diameter long pipe to ensure a fully developed turbulent inlet flow, Castro (1994). In the turbulent sudden expansion flow the recirculation length is mostly determined by the turbulence field. The perturbation to the flow brought about by the expansion is so strong that the turbulence generated in the shear layer dominates the influence of the inlet condition upon mean flow. Therefore, it is not surprising to see that there are no major differences between the present Newtonian measurements and those of Pak et al and other researchers (Fig. 6), in spite of different inlet conditions. However, the inlet turbulence flow field influences the turbulence in the core of the flow just downsteam of the expansion, but this effect is not strong enough to radically modify the mean flow.

This is why the mean flow behaviour of the Carbopol and Tylose solutions are similar. In order to get as strong an influence on the recirculation bubble length as that reported by Pak et al., a very elongationally elastic fluid, that changes dramatically the turbulence pattern in the shear layer, such as polyacrylamide or polyethylene oxide, is required. On the contrary, if the effect of elongational elasticity is to strongly enhance inlet condition differences this conclusion is wrong,

so that further measurements with the same fluids under different upstream conditions would be necessary to clarify this point. However, this type of strong direct elastic effect on mean flow does not exist at these high Reynolds number flows which are dominated by inertia, although they exist and are very strong in those laminar flows with rapid changes of geometry which are not affected by inertial forces, as shown by Boger and Walters (1994) and Walters and Webster (1982), amongst others.

This work shows that the elastic effects present in the turbulent sudden expansion flow are similar to those present in turbulent pipe flow, i.e., a molecular stretching effect promoted by the turbulence, and called here elongational elasticity, dampens the turbulence within the shear layer, especially its transverse components; this is not an entrance effect, except that the same elongational elasticity has also affected the turbulence in the inlet flow, which only persists in the central region of the duct for the first two diameters of the sudden expansion, the effect disappearing further downstream as the turbulence generated at the shear layer diffuses across the pipe. Therefore, we must conclude that the longer recirculations of the polyacrylamide solutions, as compared to the Carbopol data of Pak et al. and our Tylose measurements, must result from a very strong dampening of turbulence after the sudden expansion, much more intense than measured here with the Tylose. This is not surprising, because polyacrylamide is known, together with polyethylene oxide, as one of the best available drag reducer polymers. As mentioned before, Kostic (1994a) has also reported that some Carbopol solutions, although exhibiting shear elasticity in rheological measurements, are known to behave in turbulent pipe flow as purely viscous fluids, showing no drag reduction, i.e., showing negligible elongational elasticity, and so would not exhibit any significant turbulence dampening relative to the water turbulent sudden expansion flow. This is consistent with the sudden expansion hydrodynamics of the Carbopol solutions reported by Pak et al. (1990) and the measurements, the theories and conclusions developed in this work.

It must be stated here that all these arguments and conclusions are based on a wide acceptance of the theory relating turbulent pipe flow drag reduction and elongational elasticity. There is no direct rheological evidence of the relationship between drag reduction and elongational elasticity of dilute polymer solutions as well as of dilute viscoelastic fluids exhibiting a negligible elongational elasticity. All the existing experimental and numerical evidence is indirect, relying on laminar flows, on the behaviour of more concentrated solutions and on rheological models which are known to have a limited application.

To finalise, this work shows that future research on expansion flows should be aimed at confirming some of these conclusions, measuring the turbulence flow field with purely viscous, slightly elastic and very elastic fluids, and investigating the effects of expansion ratio and inlet flow condition. The flow behaviour at transitional Reynolds numbers for different non-Newtonian fluids should also be looked at. However, it will be the future development of a reliable elongational rheometer for low viscosity fluids that will contribute most to increase the understanding of non-Newtonian turbulent flow characteristics.

5 Conclusions

Mean and turbulent velocity flow characteristics of shear-thinning, low molecular weight polymer solutions of low shear elasticity were measured in an axisymmetric sudden expansion.

The recirculation bubble length of the 0.4% Tylose solutions was seen to be reduced by 10% compared to the water flow for Reynolds numbers above 12,000, but a decrease in the Reynolds number below this value was seen to increase its size again. However, the observed changes in mean flow were not so significant as those reported by Pak et al. (1990) in their comparison between inelastic and very elastic fluids.

In spite of the low shear elasticity of these fluids, reductions of 7, 14 and 30% were observed in the axial, tangential and radial components of the normal Reynolds stresses between the 0.4% Tylose flow at Reynolds number of 12,000 and the water flow at a Reynolds number of 178,000. This dampening of turbulence was seen to be less intense than that reported with more elastic fluids in the flow downstream of a confined baffle of Pinho and Whitelaw (1991), and showed that the elongational elasticity of these solutions was not negligible.

It was also concluded that the large lengthening of the recirculation bubble of very elastic fluids, such as polyacrylamide solutions, reported by Pak et al. (1990) must be associated with a very strong dampening of turbulence within the shear layer downstream of the sudden expansion, especially in the transverse directions, as happens in wall flow with the same fluids.

Finally, the important role of elongational viscosity on turbulent flow phenomena and the very limited or almost non-availability of this measurement in standard commercial rheometrical equipment, together with the difficult interpretation of its experimental data whenever available, means that in future non-Newtonian turbulent flow investigations, the researchers should attempt to characterise the elongational elasticity of the fluids indirectly in a well known flow, for instance via friction factor measurements in a turbulent pipe flow.

References

Abbott DC; Kline, SJ (1962) Experimental investigation of subsonic turbulent flow over single and double backward facing steps. ASME J Basic Eng 84: 317–325

Back LH; Roschke EJ (1972) Shear-layer flow regimes and wave instabilities and reattachment lengths downstream of an abrupt circular channel expansion. ASME J Appl Mech Sept. 677–681

Berman NS; Tan H (1985) Two-component laser-doppler velocimeter studies of submerged jets of dilute polymer solutions. AICHE J 2: 208–215

Boger DV; Walters K (1994) Private communication on "The influence of asymmetric inlet conditions on viscoelastic flow through contractions". 1994 Lecture Series Programme of the von Karman Institute for Fluid Dynamics on "Non-Newtonian Fluid Mechnanics"

Castro OS (1994) Non-Newtonian turbulent flow in a sudden expansion. MSc. Thesis (in Portuguese). University of Porto, Portugal

Cherdron W; Durst F; Whitelaw JH (1978) Asymmetric flows and instabilities in symmetric ducts with sudden expansions. J Fluid Mech 84: 13–31

Cherry NJ; Hillier R; Latour MEMP (1984) Unsteady measurements in a separated and reattaching flow. J Fluid Mech 144: 13–46

Dimaczek G; Tropea C; Wang AB (1989) Turbulent flow over two-dimensional surface-mounted obstacles: plane and axisymmetric geometries. In: Advances in Turbulence 2, Springer Verlag, Heidelberg.

Durrett RP; Stevenson WH; Thompson HD (1988) Radial and axial turbulent flow measurements with an LDV in an axisymmetric sudden expansion air flow. ASME J Fluids Eng 110: 367–372

Durst F; Melling A; Whitelaw JH (1981) Principles and Practice of Laser-Dopper Anemometer, 2nd edition, Academic Press, London

Freeman AR (1975) Laser anemometer measurements in a recirculating region downstream of a sudden pipe expansion. Proceedings of the LDA Symposium, Copenhagen, pp 704–709

Halmos AL; Boger DV (1975) The behaviour of a power law fluid flowing through a sudden expansion. Part II. Experimental verification. AICHE J 21: 550–553

Halmos AL; Boger DV; Cabelli A (1975) The behaviour of a power law fluid flowing through a sudden expansion. Part I. Numerical solution. AICHE 21: 540–549

Hinch EJ (1977) Mechanical models of dilute polymer solutions in strong flows. Phys Fluids 20: S22–S30

Hoyt JW (1972) The effect of additives on fluid friction. ASME J Basic Eng 94: 258–285

Iribarne A; Frantisak F; Hummel RL; Smith JW (1972) An experimental study of instabilities and other flow properties of a laminar pipe jet. AICHE J 18: 689–698

Kalinske AA (1946) Conversion of kinetic to potential energy in flow expansions. Trans ASCE 355–359

Khezzar L; Whitelaw JH; Yianneskis M (1985) An experimental study of round sudden expansion flows. Proc. 5th Symp. on Turb. Shear Flows. Cornell University: 5–25

Kostic M (1994a) On turbulent drag and heat transfer reduction phenomena and laminar heat transfer enhancement in non-circular duct flow of certain non-Newtonian fluids. Int J Heat Mass Transfer 37: 133–147

Kostic M (1994b). Different non-Newtonian Reynolds and Prandtl numbers: their usage and relationships. ASME Symposium on "Developments in Non-Newtonian Flows II", FED Vol. 206 & AMD Vol. 191: 163–169

Kozicki W; Chou CH; Tiu C (1966) Non-Newtonian flow in ducts of arbitrary cross sectional shape. Chem Eng Sci 21: 665–679

Koziol K; Glowacki P (1989) Turbulent jets of dilute polymer solutions. J Non-New Fluid Mech 32: 311-328

Luchik TS; Tiederman WG (1988) Turbulent structure in low concentration drag-reducing channel flows. J Fluid Mech 190: 241–263

Mecagno EO; Hung TK (1966) Computation and experimental study of a captive annular eddy. J Fluid Mech 28: 43–64

Moon LF; Rudinger G (1977) Velocity distribution in an abruptly expanding circular duct. ASME J Fluids Eng 99: 226–230

Pak B; Cho YI; Choi SU (1990) Separation and reattachment of non-Newtonian fluid flows in a sudden expansion pipe. J Non-Newt Fluid Mech 37: 175–179

Pak B; Cho YI; Choi SU (1991) Turbulent hydrodynamic behavior of a drag-reducing viscoelastic fluid in a sudden expansion pipe. J Non-Newt Fluid Mech 39: 353–373

Pereira AS; Pinho FT (1994) Turbulent pipe flow characteristics of low molecular weight polymer solutions. J Non-Newt Fluid Mech 55: 321

Perera MGN; Walters K (1977) Long range memory effects in flows involving abrupt changes in geometry. Part 2: The expansion/contraction/expansion Problem. J Non-Newt Fluid Mech 2: 191–204

Pinho FT; Whitelaw JH (1991) Flow on non-Newtonian fluids over a confined baffle. J. Fluid Mech 226: 475–496

Politis S (1989) Turbulence Modelling of Inelastic Power-Law Fluids. Brite report RIIB.0085.UK(H)-Technical report 52 Imperial College, London

Restivo AO; Whitelaw JH (1978) Turbulence Characteristics of the Flow Donstream of a Symmetric, Plane, Sudden Expansion. ASME J Fluids Eng 100: 308–310

Stieglmeier M; Tropea C (1992) A miniaturized, mobile laser-doppler anemometer. Appl Optics 111: 4096–4099

Stieglmeier M; Tropea C; Weiser N; Nitsche W (1989) Experimental investigation of the flow through axisymmetric expansions. ASME J Fluids Eng 111: 464–471

Townsend P; Walters K (1994) Expansion flows of non-Newtonian liquids. Chem Eng Sci 49: 749–763

Virk PS (1975) Drag reduction fundamentals. AICHE J 21: 625–656

Walters K; Webster MF(1982) On dominating elastico-viscous response in some complex flows. Phil Trans Roy Soc London A 308: 199–218